

BEDFORD.



MINISTRY OF AVIATION

AERONAUTICAL RESEARCH COUNCIL

CURRENT PAPERS

Pressure Measurements on
a Cone-Cylinder-Flare
Configuration at Small
Incidences for $M_\infty = 6.8$

by

J. G. Woodley

LONDON: HER MAJESTY'S STATIONERY OFFICE

1963

PRICE 2s 6d NET

March, 1961

PRESSURE MEASUREMENTS ON A CONE-CYLINDER-FLARE
CONFIGURATION AT SMALL INCIDENCES FOR $M_{\infty} = 6.8$

by

J. G. Woodley

SUMMARY

Pressure measurements were made on a slender cone-cylinder-flare configuration, slightly blunted at the nose, for 0, 3 and 6 degrees incidence at a free-stream Mach number of 6.8.

It was found that the surface pressures obtained on the cone agreed with extrapolations to $M_{\infty} = 6.8$ of theoretical values given in M.I.T. Tables³ (Kopal) for yawed cones, and that Impact theory gave a good indication of the pressure level to be expected on all parts of the body where surface incidence was sufficiently large to merit its use.

The semi-angles of the conical and flared parts of the model were both $7\frac{1}{2}$ degrees, and, as was expected, along each generator of the body the pressure level on the flare rose in all cases to approximately that developed upstream on the cone surface.

No evidence of a marked over-expansion to pressures below the free-stream value was noticed at the junction between cone and cylinder.

LIST OF CONTENTS

	<u>Page</u>
1 INTRODUCTION	3
2 TUNNEL AND MODEL	3
2.1 Tunnel	3
2.2 Model	3
3 SYSTEMS FOR PRESSURE MEASUREMENT AND TESTING TECHNIQUES	3
3.1 Stagnation pressure	3
3.2 Static pressure on the model	3
3.2.1 Pressure response and testing technique	4
4 EXPERIMENTAL RESULTS	4
4.1 Pressures on the conical part of the body	4
4.2 Pressures on the cylindrical part of the body	5
4.3 Pressures on the conical flare	5
5 CONCLUSIONS	5
LIST OF SYMBOLS	6
LIST OF REFERENCES	7
TABLE 1	8
ILLUSTRATIONS - Figs.1-3	-
DETACHABLE ABSTRACT CARDS	-

LIST OF ILLUSTRATIONS

	<u>Fig.</u>
Diagram of the cone-cylinder-flare model showing position of the pressure-holes	1
The electromanometer system	2
(a) Pressure distribution at zero incidence ($M_{\infty} = 6.8$)	
(b) Pressure distribution at 3° incidence ($M_{\infty} = 6.8$)	
(c) Pressure distribution at 6° incidence ($M_{\infty} = 6.8$)	3

1 INTRODUCTION

The current search for shapes which might be suitable for hypersonic vehicles has suggested the cone-cylinder-flare configuration as one of the possible shapes.

Theoretical methods available at present for predicting the pressure distributions and resultant forces at hypersonic speeds on such bodies of revolution are limited to the case of flow at zero or small incidence. For larger incidences, one is forced to lean rather heavily on Newtonian Impact theory or empirical generalisations based on it. Systematic experimental information is required, therefore, to check the adequacy of the various methods of prediction and, if discrepancies occur, to check on the causes of such discrepancies.

In the present tests, pressure measurements were made on a slender cone-cylinder-flare body, which was slightly blunted at the nose, at 0, 3, and 6 degrees incidence at a free-stream Mach number of 6.8. It is intended to follow these soon by force and pressure measurements on similar models at the same Mach number for incidences up to about 30 degrees.

2 TUNNEL AND MODEL

2.1 Tunnel

The 7" x 7" Hypersonic wind tunnel at R.A.E./Farnborough was used for these tests. Details of the design and performance of this facility for operation at a Mach number of 6.8 are given in Refs.1 and 2. The stagnation pressure in these tests was about 52 atmospheres and the stagnation temperature was approximately 650°K. The stagnation conditions correspond to a free-stream Reynolds number of 0.5 million per inch.

2.2 Model

The model, shown in Fig.1, was a cone-cylinder-flare made of stainless steel. The semi-angles of the cone and the conical flared-portion were both $7\frac{1}{2}^{\circ}$, and the model had spherical blunting at the nose. Fifteen of the seventeen pressure holes available were concentrated along one generator of the body, and flexible pressure-tube connections were used in the sting support so that the pressure distribution around the body could be obtained by rotating the model about its axis.

3 SYSTEMS FOR PRESSURE MEASUREMENT AND TESTING TECHNIQUES

3.1 Stagnation pressure

The method used for measurement of this pressure is given in detail in Ref.1. For these tests the stagnation pressure was held to within ± 0.5 p.s.i. at a level around 765 p.s.i. (abs) and was measured to an accuracy of 0.01%.

3.2 Static pressure on the model

A block diagram of the electromanometer-system used for measuring surface pressures on the model is shown in Fig.2. (For details of components, see Ref.1.)

In this diagram the part of the system used to record the surface pressure is shown outside the dashed rectangle. During a test these pressures are individually selected at the Scanivalve (a rotary pressure switch), and are recorded on a Honeywell-Brown recorder through the transducer system,

which is referred to vacuum. The transducer used for the present tests had a linear output with a full scale deflection on the recorder of 1.5 p.s.i. The resulting accuracy of pressure measurement is considered to be of the order ± 0.005 p.s.i.

The part of the system shown inside the dashed rectangle is used to calibrate the transducer. For this, a dead-weight tester, which is evacuated to give an absolute measure of pressure, is set for a particular pressure. It is then used to monitor the adjustment of a reservoir to this pressure. Pressure control in the reservoir, which in turn is connected to the transducer, is obtained through a coarse bleed to a vacuum pump and a fine bleed in from atmosphere through a needle valve. Once the reservoir pressure has been correctly set in this way the transducer output is recorded.

Calibration by this method verified the linearity of the output from the transducer used for the present tests over the whole of its range.

3.2.1 Pressure response and testing technique

Since several surface pressures had to be recorded consecutively on the transducer during a run, the Scanivalve was connected to the transducer by very short leads, in order to reduce the volume of air which had to be adjusted to each new pressure. Connections from the model to the Scanivalve were also made as short as possible. However, in order to allow for the rotation of the model about its axis, mentioned in Section 2.2, it was necessary to use some small bore rubber tubing for connections to the model inside the sting support. In addition to this, the bore of the holes through the Scanivalve itself was also small. Hence rather a large pressure lag occurred in the system, resulting in a response of about 5 seconds.

Because of the high convective heat transfer to the model during a run, the use of rubber tubing inside the sting restricted the length of each tunnel run to about 45 seconds, whereas without this restriction a run of up to 3 minutes would have been possible.

The combined effect of these limitations was that only 7 surface pressures could be recorded during each run, by manual selection at the Scanivalve. Hence, the technique adopted for measuring the surface pressures at the 17 positions available on the model was to make three identical runs and read 7 surface pressures each time. This system allowed an overlap of two readings between both the first and second runs, and the second and third runs of each set, in order to check the consistency of the results.

4 EXPERIMENTAL RESULTS

The pressure distributions on the model, obtained at 0° , 3° , and 6° incidence, for particular values of the meridional angle ϕ (measured from the plane of symmetry on the windward side of the body) are given in Table 1 both as p/p_0 (ratio of surface pressure to free stream stagnation pressure) and as C_p (pressure coefficient) versus s/D (ratio of distance from the nose along the surface to the diameter of the cylinder). These results are illustrated in Figs.3(a), (b), (c).

4.1 Pressure on the conical part of the body

In Figs.3 the surface pressures on the cone are compared to the theoretical values obtained for the case of a sharp cone from M.I.T. Tables³ (Kopal) by extrapolating the results to a Mach number of 6.8. Further comparison is made by including also estimates obtained both from Impact

(Newtonian) theory and its modification given in Ref.4, for the cases* in which they might reasonably be applied.

It is of note that, for these cases* where its results are expected to be applicable, Impact theory gives a reasonable estimate, even though in general it is an underestimate, of the pressure on the cone.

4.2 Pressures on the cylindrical part of the body

At zero incidence Fig.3(a) shows that the surface pressure on the cylinder is reduced downstream of the cone-cylinder junction from its value on the cone to about free-stream pressure (i.e. $C_p = 0$) within the length of the diameter (D) of the cylinder. In other words, the pressure on the cylinder induced by the presence of the cone decays to zero inside one diameter from the junction. It is also of note that there is no evidence of an over-expansion of Prandtl-Meyer type from the cone to the cylinder as is predicted by the characteristics solutions of Ref.5.

When at incidence, Figs.3(b) and (c), the pressure on each meridian generator again follows the above trend, with a decrease from its value on the cone to some uniform level on the cylinder within a length D from the cone-cylinder junction. In each of these Figs. the results from both Impact and modified Impact theory⁴ have been included where they might be applicable*. (i.e. for only the most windward generator ($\phi = 0$) at 3 and 6 degrees incidence). Fair agreement can be seen between the theoretical results and the experimental values for the central part of the cylinder's surface, where, as before in the case of the cone, the theoretical values tend to underestimate the surface pressure.

4.3 Pressures on the conical flare

For each generator the pressures on the flare, as can be seen from Figs.3, rose approximately to the same level as on the cone, within a distance D from the cylinder-flare junction. The pressure level on the cone would be expected to form the upper limit for the pressure developed on the flare in this manner, since the semi-angles of the cone and flare were equal in these tests.

Results for pressures on the flare calculated by Impact theories⁴ are also shown in Figs.3. In general poorer agreement with the pressure levels of the experimental results is found for the modified version of Impact theory than for the basic theory itself. However, it should be pointed out in this context that the modified theory was developed strictly for the case of larger angles of surface incidence, η , than occurred in the present tests.

5 CONCLUSIONS

Pressure measurements made at a Mach number of 6.8 on a cone-cylinder-flare configuration at incidences of 0, 3 and 6 degrees gave the following results.

- (1) Pressures on the cone were predicted reasonably well, though in general underestimated, by Impact (Newtonian) theory for all surface incidences where this type of theory could reasonably be expected to apply.

* Ref.4 suggests the lower limit for the application of Impact theory as $M_\infty \eta > 0.3$, where M_∞ is the free-stream Mach number and $(\pi/2 - \eta)$ is the angle between the surface normal and the free stream direction at the point considered.

Good agreement was obtained in all cases with theoretical values which were calculated from M.I.T. Tables³ of flow around yawed cones, (by extrapolation of the results given therein to a Mach number of 6.8).

(2) Pressures measured on the cylinder gave no indications of marked over-expansion immediately downstream of the cone-cylinder junction. Such over-expansion should have occurred if the expansion at this junction was of Prandtl-Meyer type. Impact theory gave a reasonable estimate of the pressure level to be expected on the cylinder whenever the surface incidence, η , was large enough for this type of theory to apply.

(3) For each generator the pressures on the flare rose in all cases from the level on the cylinder to a level equal to that developed on the cone.

LIST OF SYMBOLS

M_∞ free stream Mach number

p surface pressure on body

p_∞ free stream static pressure

p_o free stream stagnation pressure

C_p surface pressure coefficient $\left(= \frac{p - p_\infty}{\gamma/2 p_\infty M_\infty^2} \right)$

γ ratio of specific heats for air (= 1.4)

α angle of incidence of the model (degrees)

ϕ meridional angle measured in the cross-sectional plane of the body relative to the most windward generator (radians)

η surface incidence at a particular point (i.e. $(\pi/2 - \eta)$ is the angle between the surface normal and the free stream direction) (radians)

s distance along the model surface measured from the stagnation point (inches)

D diameter of the cylindrical part of the body (= 1.28 inches)

LIST OF REFERENCES

<u>Ref.No.</u>	<u>Author(s)</u>	<u>Title, etc.</u>
1	Crabtree, L.F. Crane, J.F.W.	The 7 in. x 7 in. Hypersonic Wind Tunnel at R.A.E./Farnborough. Part I. Design, Instrumentation and flow visualization techniques. A.R.C. C.P.590. August, 1961
2	Crane, J.F.W.	The 7 in. x 7 in. Hypersonic Wind Tunnel at R.A.E./Farnborough. Part II. Heater Performance. A.R.C. C.P.590. August, 1961
3	Kopal, Z. (Ed)	Tables of supersonic flow around yawing cones. M.I.T. Center of Analysis Technical Report No.3 1947
4	Collingbourne, J.R. Crabtree, L.F. Bartlett, W.J.	A modification of Impact theory for the prediction of pressures on bodies of revolution at high supersonic and hypersonic speeds. ($M > 3$) Unpublished M.o.A. Report.
5	Clippinger, Giese, Carter	Tables of supersonic flow about cone-cylinders Pt.I. Surface Data B.R.L. Report No.729 July 1950

TABLE 1 (Contd.)

	α°	6		6		6	
		ϕ (radians)		π		$\pi/2$	
		s/D	$\frac{p}{p_0} \times 10^4$	$C_P \times 10^2$	$\frac{p}{p_0} \times 10^4$	$C_P \times 10^2$	$\frac{p}{p_0} \times 10^4$
Cone	1.78	12.9	10.6	4.3	1.5	5.6	2.9
	2.17	13.2	11.0	4.3	1.5	6.0	3.3
	2.57	13.6	11.4	4.1	1.3	6.0	3.3
	2.97	13.6	11.4	4.1	1.3	6.4	3.7
	3.35	7.2	4.6	3.7	0.9	4.6	1.8
Cylinder	3.75	5.7	3.0	3.2	0.3	3.0	0.1
	4.15	5.6	2.9	3.1	0.2	2.7	-0.2
	4.54	5.5	2.8	2.7	-0.2	2.5	-0.4
	4.92	5.3	2.6	2.8	-0.1	2.5	-0.4
	5.32	5.3	2.6	2.8	-0.1	2.5	-0.4
Flare	5.71	6.7	4.0	2.8	-0.1	-	-
	6.09	10.9	8.5	4.0	1.2	4.8	2.0
	6.49	13.2	11.0	4.0	1.2	5.8	3.1
	6.89	12.5	10.2	4.0	1.2	6.0	3.3
	7.28	12.2	9.8	4.1	1.3	6.0	3.3

$\frac{a}{D} = 3.31$

$\frac{a}{D} = 5.92$

TABLE 1

		α°	0		3		3	
		ϕ (radians)	—		0		π	
		s/D	$\frac{p}{p_0} \times 10^4$	$C_P \times 10^2$	$\frac{p}{p_0} \times 10^4$	$C_P \times 10^2$	$\frac{p}{p_0} \times 10^4$	$C_P \times 10^2$
$D/s = 3.31$	Cone	1.78	6.2	3.5	8.9	6.4	4.5	1.7
		2.17	6.4	3.7	9.4	6.9	4.6	1.8
		2.57	6.4	3.7	9.3	6.8	4.6	1.8
		2.97	6.5	3.8	9.7	7.2	5.1	2.4
		3.35	4.9	2.1	5.7	3.0	4.2	1.4
		3.75	3.5	0.7	4.3	1.5	3.1	0.2
$D/s = 5.92$	Cylinder	4.15	3.1	0.2	4.0	1.2	2.8	-0.1
		4.54	3.1	0.2	3.8	1.0	2.7	-0.2
		4.92	3.0	0.1	3.7	0.9	2.7	-0.2
		5.32	3.1	0.2	3.6	0.8	2.7	-0.2
		5.71	3.4	0.6	3.7	0.9	3.0	0.1
Flare	6.09	3.7	0.9	7.0	4.3	3.1	0.2	
	6.49	4.5	1.7	9.5	7.0	3.4	0.6	
	6.89	5.7	3.0	9.3	6.8	3.8	1.0	
	7.28	5.9	3.2	9.3	6.8	4.2	1.4	

TABLE 1 (Contd.)

α°	6		6		6		
	$\frac{P}{P_0} \times 10^4$	$C_F \times 10^2$	$\frac{P}{P_0} \times 10^4$	$C_F \times 10^2$	$\frac{P}{P_0} \times 10^4$	$C_F \times 10^2$	
ϕ (radians)	0		π		$\pi/2$		
s/D	$\frac{P}{P_0} \times 10^4$	$C_F \times 10^2$	$\frac{P}{P_0} \times 10^4$	$C_F \times 10^2$	$\frac{P}{P_0} \times 10^4$	$C_F \times 10^2$	
Cone	1.78	12.9	10.6	4.3	1.5	5.6	2.9
	2.17	13.2	11.0	4.3	1.5	6.0	3.3
	2.57	13.6	11.4	4.1	1.3	6.0	3.3
	2.97	13.6	11.4	4.1	1.3	6.4	3.7
	3.35	7.2	4.6	3.7	0.9	4.6	1.8
Cylinder	3.75	5.7	3.0	3.2	0.3	3.0	0.1
	4.15	5.6	2.9	3.1	0.2	2.7	-0.2
	4.54	5.5	2.8	2.7	-0.2	2.5	-0.4
	4.92	5.3	2.6	2.8	-0.1	2.5	-0.4
	5.32	5.3	2.6	2.8	-0.1	2.5	-0.4
Flare	5.71	6.7	4.0	2.8	-0.1	-	-
	6.09	10.9	8.5	4.0	1.2	4.8	2.0
	6.49	13.2	11.0	4.0	1.2	5.8	3.1
	6.89	12.5	10.2	4.0	1.2	6.0	3.3
	7.28	12.2	9.8	4.1	1.3	6.0	3.3

$\frac{s}{D} = 3.31$

$\frac{s}{D} = 5.92$

NOSE RADIUS = 0.125"

DIAMETER OF CYLINDER (D) = 1.28"

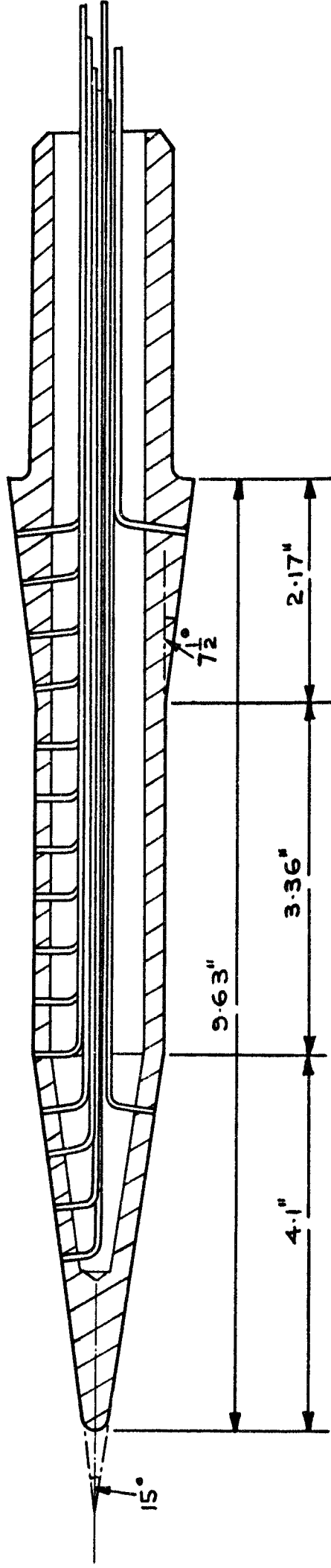


FIG.1. DIAGRAM OF THE CONE-CYLINDER-FLARE MODEL SHOWING POSITIONS OF THE PRESSURE-HOLES.

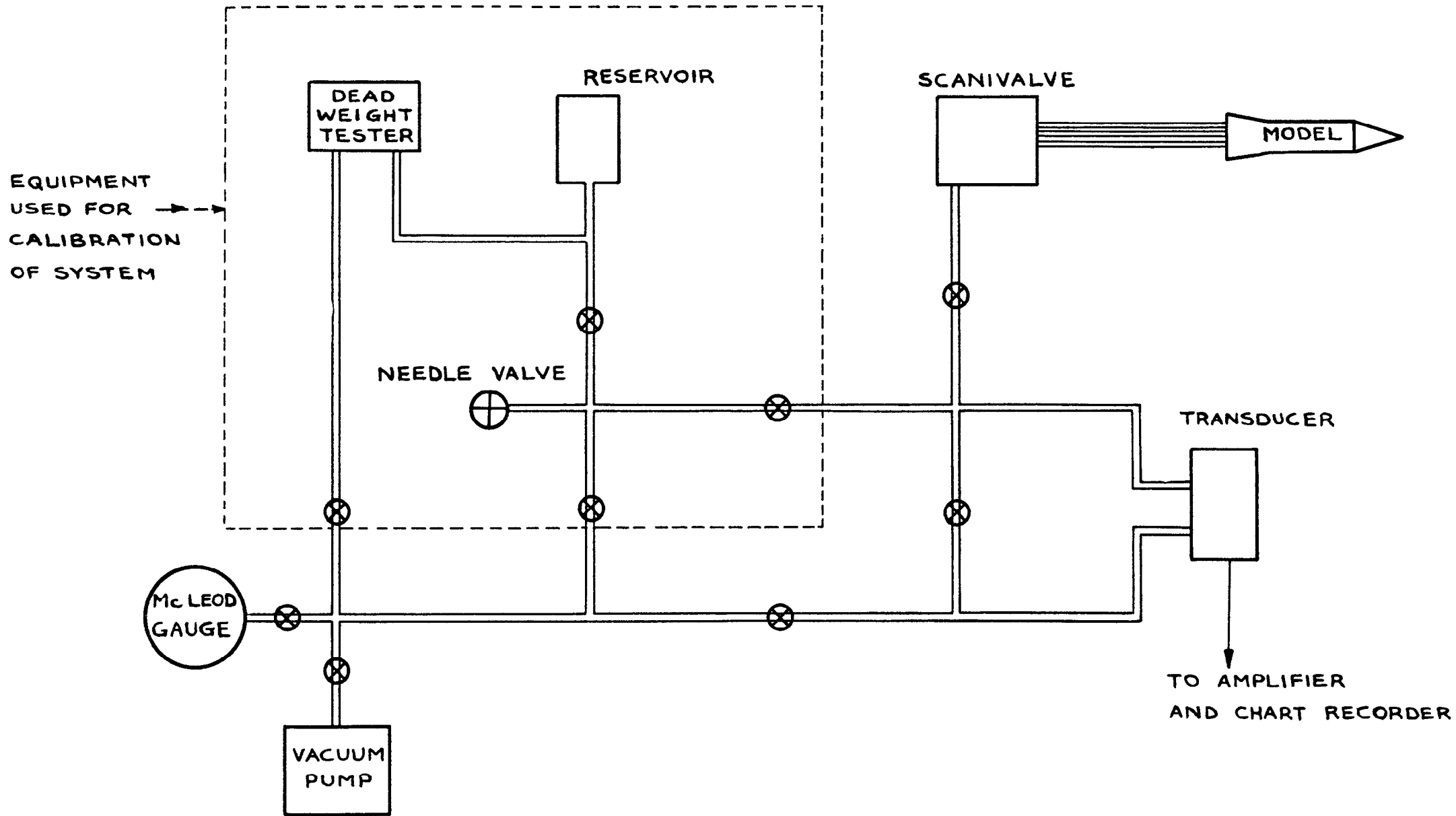


FIG. 2. THE ELECTROMANOMETER SYSTEM

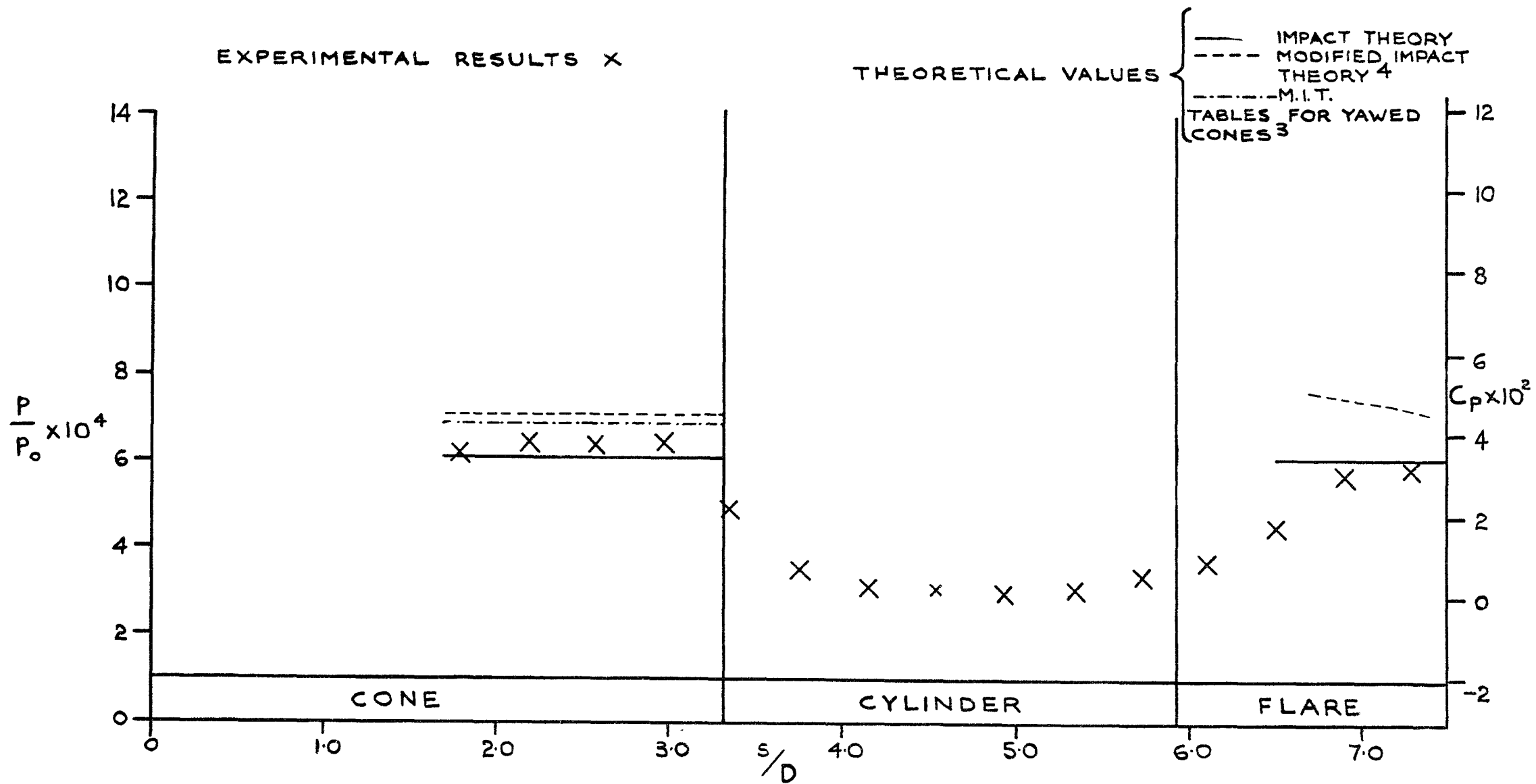


FIG.3 (a) PRESSURE DISTRIBUTION AT ZERO INCIDENCE. ($M_\phi = 6.8$)

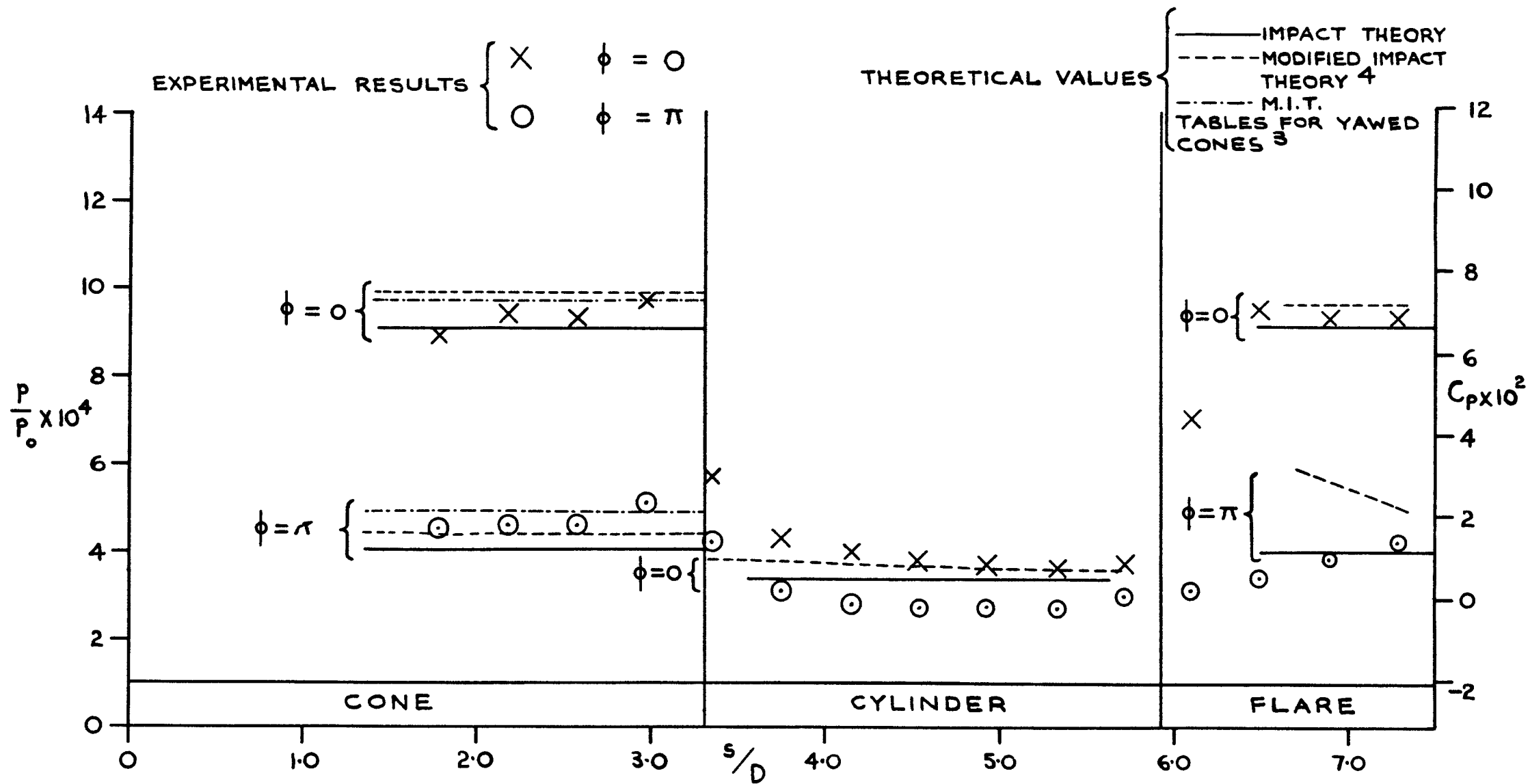


FIG.3(b). PRESSURE DISTRIBUTIONS AT 3° INCIDENCE. ($M_\phi = 6.8$)

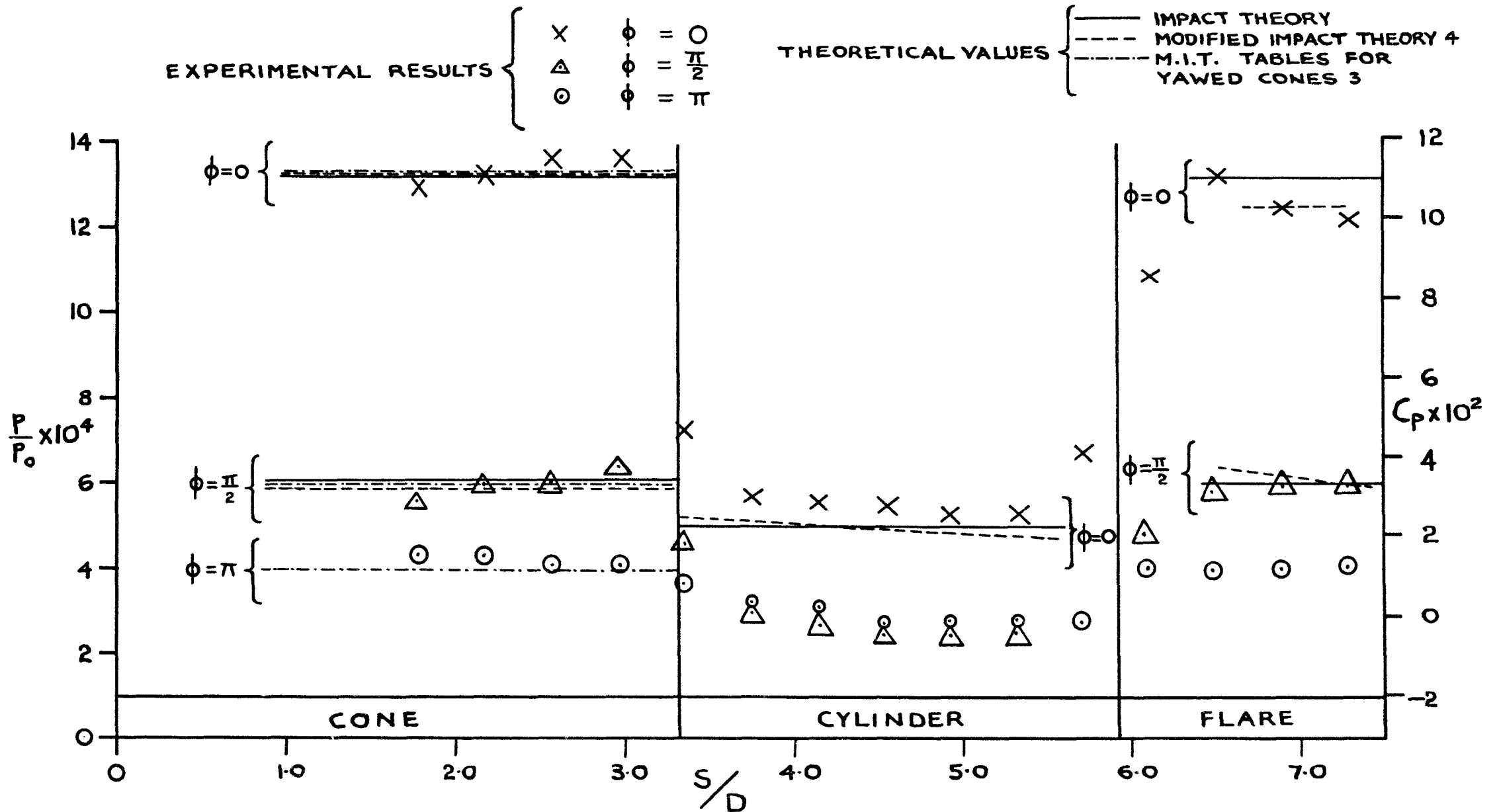


FIG. 3 (c) PRESSURE DISTRIBUTIONS AT 6° INCIDENCE. ($M_\infty = 6.8$)

A.R.C. C.P. No.632

533.696.5
533.6.011.55
533.6.048.2

PRESSURE MEASUREMENTS ON A CONE-CYLINDER-FLARE
CONFIGURATION AT SMALL INCIDENCES FOR $M_\infty = 6.8$
Woodley, J.G. March, 1961

Pressure measurements were made on a slender
cone-cylinder-flare configuration, slightly blunted at the nose,
for 0, 3 and 6 degrees incidence at a free-stream Mach number of 6.8.

It was found that the surface pressures obtained on the cone
agreed with extrapolations to $M_\infty = 6.8$ of theoretical values given in
M.I.T. Tables³ (Kopal) for yawed cones, and that Impact theory gave a
good indication of the pressure level to be expected on all parts of the
body where surface incidence was sufficiently large to merit its use.

(Over)

A.R.C. C.P. No.632

533.696.5
533.6.011.55
533.6.048.2

PRESSURE MEASUREMENTS ON A CONE-CYLINDER-FLARE
CONFIGURATION AT SMALL INCIDENCES FOR $M_\infty = 6.8$
Woodley, J.G. March, 1961

Pressure measurements were made on a slender
cone-cylinder-flare configuration, slightly blunted at the nose,
for 0, 3 and 6 degrees incidence at a free-stream Mach number of 6.8.

It was found that the surface pressures obtained on the cone
agreed with extrapolations to $M_\infty = 6.8$ of theoretical values given in
M.I.T. Tables³ (Kopal) for yawed cones, and that Impact theory gave a
good indication of the pressure level to be expected on all parts of the
body where surface incidence was sufficiently large to merit its use.

(Over)

A.R.C. C.P. No.632

533.696.5
533.6.011.55
533.6.048.2

PRESSURE MEASUREMENTS ON A CONE-CYLINDER-FLARE
CONFIGURATION AT SMALL INCIDENCES FOR $M_\infty = 6.8$
Woodley, J.G. March, 1961

Pressure measurements were made on a slender
cone-cylinder-flare configuration, slightly blunted at the nose,
for 0, 3 and 6 degrees incidence at a free-stream Mach number of 6.8.

It was found that the surface pressures obtained on the cone
agreed with extrapolations to $M_\infty = 6.8$ of theoretical values given in
M.I.T. Tables³ (Kopal) for yawed cones, and that Impact theory gave a
good indication of the pressure level to be expected on all parts of the
body where surface incidence was sufficiently large to merit its use.

(Over)

The semi-angles of the conical and flared parts of the model were both $7\frac{1}{2}$ degrees, and, as was expected, along each generator of the body the pressure level on the flare rose in all cases to approximately that

No evidence of a marked over-expansion to pressures below the free-stream value was noticed at the junction between cone and cylinder.

The semi-angles of the conical and flared parts of the model were both $7\frac{1}{2}$ degrees, and, as was expected, along each generator of the body the pressure level on the flare rose in all cases to approximately that developed upstream on the cone surface.

No evidence of a marked over-expansion to pressures below the free-stream value was noticed at the junction between cone and cylinder.

The semi-angles of the conical and flared parts of the model were both $7\frac{1}{2}$ degrees, and, as was expected, along each generator of the body the pressure level on the flare rose in all cases to approximately that developed upstream on the cone surface.

No evidence of a marked over-expansion to pressures below the free-stream value was noticed at the junction between cone and cylinder.

C.P. No. 632

© *Crown Copyright 1963*

Published by
HER MAJESTY'S STATIONERY OFFICE

To be purchased from
York House, Kingsway, London w.c.2
423 Oxford Street, London w.1
13A Castle Street, Edinburgh 2
109 St. Mary Street, Cardiff
39 King Street, Manchester 2
50 Fairfax Street, Bristol 1
35 Smallbrook, Ringway, Birmingham 5
80 Chichester Street, Belfast 1
or through any bookseller

Printed in England

S.O. CODE No. 23-9013-32

C.P. No. 632